Contribution of combustion to the blast wave strength after high-pressure hydrogen tank rupture in a fire

Molkov V.V., Cirrone D.M.C., Shentsov V.V., Dery W., Makarov D.V.
Ulster University, Hydrogen Safety Engineering and Research Centre (HySAFER)
Newtownabbey, Co. Antrim, BT37 0NL, Northern Ireland, UK

1 Introduction

Fuel cell vehicles store hydrogen onboard at pressure either 70 MPa (bikes, cars and tracks) or 35 MPa (buses). Tank volume is 10-140 litres. More than 1/3 of CNG car tank ruptures in a fire are due to pressure relief device failure. The quantitative risk assessment of hydrogen onboard storage [1] has demonstrated that the acceptable level of risk 10^{-5} fatalities/vehicle/year can be achieved if storage tank has fire resistance rating above 47 min. This is based on the non-zero probability of thermally activated pressure relief device (TPRD) failure. The consequences of tank rupture in a fire are blast wave, fireball, projectiles. To underpin hydrogen safety engineering the underlying physical phenomena should be understood first. The aim of this study is to understand if there is a contribution of combustion into the blast wave strength.

2 Results of previous study on contribution of combustion into the blast wave strength

This work expands our previous study on the contribution of combustion carried out by the reduced physical model to the CFD model. Figure 1 shows results of the analysis of hydrogen tanks rupture in fire tests performed in USA [2-5] using the reduced model [6]. Two tests were analysed. One test with a stand-alone tank, and another test with a tank located under a vehicle. The stand-alone Type IV hydrogen storage tank length was 0.84 m, diameter 0.41 m, internal volume 72.4 L. Initial storage pressure was 34.3 MPa and temperature 300 K (1.64 kg hydrogen). At time of rupture in a fire after 6 min 27 sec of fire exposure (fire heat release rate was 350 kW) they raised to 35.7 MPa and 312.15 K respectively. Three sensors were located perpendicular to the tank axis in a straight line at distances 1.9, 4.2 and 6.5 m from the tank centre. The fourth sensor was located along the tank axis at 4.2 m. The blast wave decayed faster along the tank axis (28% reduction of overpressure from 83 kPa to 64.8 kPa at the same distance 4.2 m). The maximum reported diameter of the fireball was 7.7 m at time 45 ms after the tank rupture.

Figure 1 (left) shows that the release of only mechanical energy of compressed gas, E_m, after tank rupture (dashed line) is not enough to closely reproduce experimentally measured blast overpressure (symbols). Due

Correspondence to: v.molkov@ulster.ac.uk

to hemispherical geometry and a loss of a part of the energy to burner destruction and ground cratering the mechanical energy coefficient, α=1.8, is below ideal case value α=2.0. To reproduce experimental pressures the chemical energy is introduced into the scaling of dimensionless radius [6]. The fraction of the total chemical energy of hydrogen complete combustion that contributed to the blast wave strength, i.e. reached the leading shock by sound waves propagating through temperature descending media, is β=0.052. Thus, only 5.2% of released and burnt hydrogen contributed to the blast wave strength. The rest of hydrogen will be fully combusted in fireball in about 2 s. The released mechanical energy is estimated as 7.33 MJ and the fraction of the total chemical energy that contributed to the blast wave strength is calculated as 10.3 MJ [6].

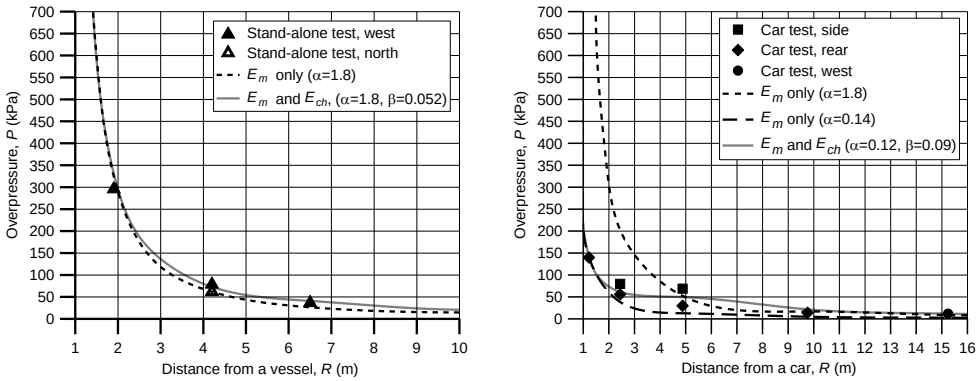

Figure 1. Left: stand-alone tank fire test; right: under-vehicle tank fire test

Figure 1 (right) demonstrates clearly that experimental blast overpressures for the case of tank rupture under the vehicle cannot be reproduced by the theory accounting for mechanical energy only [7] – please see two dashed lines – one of which underpredicts the blast pressure in the far field (if the pressure in a near field is matched, curve with α=0.14), and another hugely overpredicts the pressure in a near field (if pressure in a far field is matched, curve with α=1.8). Only the physical model [6] can reproduce experimental pressure decay, including the "plateau" of pressure at distances 3-6 m. To reproduce the experimental pressures for the under-vehicle tank, rupture the mechanical energy coefficient was found to be reduced from α=1.8 (the case of stand-alone tank) to α=0.12 (15 times!) due to significant losses of mechanical energy to demolish the car and threw it away by 22 m from its original location. However, the presence of the vehicle has increased the amount of burned hydrogen that contributed to the blast wave strength by about twice from β=0.052 to β=0.09 due to longer time of high-pressure presence in confined space under vehicle and more intensive turbulent combustion. The study [6] concluded that there is a contribution of hydrogen combustion at the contact surface behind the starting shock to the blast wave strength. However, the mechanism of combustion was not clear. This study aims to get insights into this mechanism.

3 LES model and numerical details

Large eddy simulations (LES) of shock and reacting flow are performed using Fluent as the computational engine. The pressure-based solver coupled with PISO pressure-velocity algorithm is applied. The governing equations are based on the filtered conservation equations for mass, momentum and energy in their compressible form. The ground is specified as no-slip wall. Simulations with adiabatic and non-adiabatic boundary condition at the ground didn't show difference in the pressure dynamics at sensor locations due to a short time available for heat transfer. The external non-reflecting boundary is defined as pressure outlet with zero-gauge pressure.

Hydrogen behaves as a real gas at pressures above 10 MPa. The maximum pressure beyond the tank after its rupture is in the starting shock, which is about 5 MPa for 35 MPa storage and 8 MPa for 70 MPa storage. The chemical reactions of combustion take place at the contact surface between air and hydrogen behind the starting shock. Thus, an ideal gas chemistry can be adopted for simulations. To use ideal gas in the simulations we need to scale tank volume to conserve the mechanical energy. By comparison of equations for mechanical energy of compressed ideal and real gas, a tank volume scaling to conserve the mechanical energy is: $V_{ideal} = V_{real} - mb$, where m is the mass of stored hydrogen, and b is the co-volume constant for hydrogen. For USA test [2] the volume of tank is reduced in simulations from 72.2 L to 59.5 L. For Japanese tests [8] the tank in Test 1 was scaled from 35 L to 23.9 L, and in Test 2 from 36 L to 24.6 L.

The second order scheme is used for pressure to improve simulation accuracy for compressible flows. A second order upwind scheme is used for convective terms, given that the flow is characterised by Peclet number higher than 2 ($Pe = (\rho c_p u\, \Delta x)/k$). The first order is employed for time advancement (change to the second order scheme for time advancement for the case with constant time step did not cause any difference in the pressure dynamics). The original time step adapting technique was employed to maintain a constant CFL number: a time step, Δt, changes in simulations following the in-house User Defined Function (UDF) that keeps CFL number constant. The CFL is calculated by equation CFL=$(u + c)$ Δt/Δx, where u is the flow velocity, c is the speed of sound, and Δx is the size of the control volume (CV). The UDF algorithm looks for a CV with the maximum value of CFL number and then calculates the speed of sound and extracts flow velocity in this cell. Then the UDF calculates the time step, using the specified CFL value that should not be exceeded in the simulations, by the equation Δt=CFL×Δx/$(u + c)$. The definition of CFL uses the speed of sound, c. However, in our physical problem we have another characteristic velocity, i.e. the shock propagation velocity, which is higher than the speed of sound. Thus, we should expect a solution convergence at CFL numbers below 1. In conditions of shock wave decay and thus decrease of the shock wave velocity it provides an automated increase of the time step during simulations. Thus, a significant saving of computational time compared to the constant time step simulations is achieved.

The Smagorinsky-Lilly model is used for the sub-grid scale turbulence modelling. To simulate the combustion and turbulence-chemistry interaction, the eddy-dissipation-concept (EDC) model is employed [9]. In the EDC model either detailed chemical mechanism or one-step Arrhenius chemistry for hydrogen combustion in the air can be applied. The one-step Arrhenius chemistry is applied in this study as it gives reduction of calculation time by a factor of four compared to detailed chemistry EDC model.

4 Japanese tests

Two fire tests were performed with 70 MPa tanks [8]. The blast wave pressure was recorded at 5 m and 10 m perpendicular to the tank axis. Test 1: Type IV tank of 35 L ruptured after 21 min of fire exposure (pressure in the tank was 94.54 MPa). The maximum overpressure at 5 m and 10 m was 110.5 and 23.4 kPa respectively. Test 2: Type III tank of 36 L burst at 11 min (pressure was 99.47 MPa). The maximum overpressure recorded was 74.3 kPa at 5 m and 23.4 kPa at 10 m. In Test 2, the maximum overpressure at the 5 m was 30% less than in Test 1, despite the slightly bigger volume and pressure before the tank burst.

5 Results and discussion

Figure 2 (left) shows experimental pressure transients for Japanese Test 2 at distance 5 m and 10 m from the tank and simulated pressure dynamics both without combustion and with combustion. The LES model without combustion underpredicts the experimental pressure by 40%. The LES model with combustion exactly reproduces both peaks of pressure at 5 m and 10 m. The “relatively slow rise time of pressure” in

both the non-reacting and reactive CFD simulations is a known phenomenon. It is due to the numerical requirement that in simulations all "fronts" are resolved by 3-5 CVs. A "proper" explicit shock capturing scheme, if this to be a part of non-viscous problem formulation, is possible but will "kill" proper simulation of turbulent combustion (and thus could "demonstrate" that combustion "doesn't contribute" to the blast wave strength"). The leading front of the simulated shock and oscillations at the end of the process were found to reduce with the computational grid refinement from 3 cm down to 1 cm in the vicinity of the tank. Thus, the question about whether the combustion contributes or not to the blast wave strength is answered. This is in line with our previous work carried out with the use of reduced physical model [6].

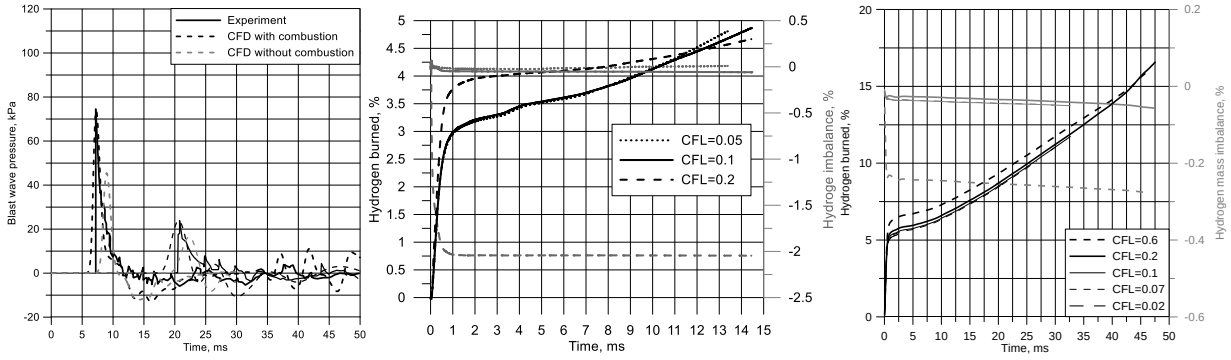

Figure 2. Pressure transients for Japanese Test 2 at location of sensors at 5 m and 10 m from the tank (left); burned hydrogen mass (black) and hydrogen mass imbalance (grey) for USA (centre) and Japanese (right) tests

Figure 2 (centre and right) shows hydrogen burned mass (black lines, left y-axis) and hydrogen mass imbalance (grey lines, right y-axis) in the computational domain as a function of time for the USA test and Japanese tests 1 and 2 (they have coinciding curves) respectively. The hydrogen mass imbalance is used as an indicator of simulations convergence by the CFL number. For both cases solution converges at CFL=0.1. The amount of hydrogen burned at the initial fast burning rate stage of duration about 1 ms is higher for Japanese tests compared to the USA test. It is due to increased pressure in the starting shock. The simulation results in Fig.2 (right) are for 2 cm mesh size in the vicinity of the tank (simulations with finer grids for the whole process are computationally prohibitive). The decrease of mesh size to 1 cm and further to 0.5 cm decreased the amount of hydrogen burnt and at 1 ms they differ by ±13% of their average value.

Figure 3 shows for the USA test simulated molar concentrations of hydrogen (H2), water vapour (H2O), and oxygen (O2), pressure and temperature distribution, and reaction rate of water vapour generation as a function of distance from the tank centre perpendicular to its axis at four moments (when drastic decrease of the combustion rate is observed): 0.1, 0.5, 1.0, and 3.0 ms. Let us analyse combustion dynamics using Fig. 2 (centre) and Fig. 3 together. The former indicates that the reaction rate is high from the start of the process and then reduces significantly as time progresses to 1-3 ms. One reason is thought to be the dilution of the reaction area at the contact surface by water vapour as the combustion product. Figure 3 shows the location of reaction zone between hydrogen and oxygen. The high temperature zone around the contact surface expands. The zone separates areas of pure hydrogen and air. It is diluted by water vapour. The reaction rate of water vapour generation is decreasing from its initial value at time 0.1-1 ms by three orders of magnitude at time 3 ms. This reduction coincides with the decrease of pressure at the contact surface by more than an order of magnitude at the same time span. The contact surface moves outwards of the tank rupture location following the shock with increasing in time distance between them. The effect of reaction zone dilution by combustion products (water vapour) seems to be not so important for the reaction rate as the effect of pressure drop in reaction zone. Indeed, relative concentration of water vapour at the contact surface is increasing but not as much to explain the reaction rate drop by 500 times.

The simulations demonstrated that due to high velocity of gases behind the starting shock the turbulent viscosity at the contact surface is 4-5 orders of magnitude higher than the laminar viscosity. This provides intensive mixing of hydrogen and air at the contact surface and thus high reaction rate contrary to a slow reaction rate between hydrogen and air in a laminar diffusion flame at atmospheric pressure. This phenomenon could be characteristic only for hydrogen tank rupture in a fire due to highest storage pressure.

The comparison of the temperature profile behind the leading shock and the reaction location shows that only a part of released chemical energy will reach the leading front and thus contribute to its magnitude. Those acoustic waves that cannot overcome the positive temperature gradient towards the leading shock will still finally contribute to the impulse of the blast wave.

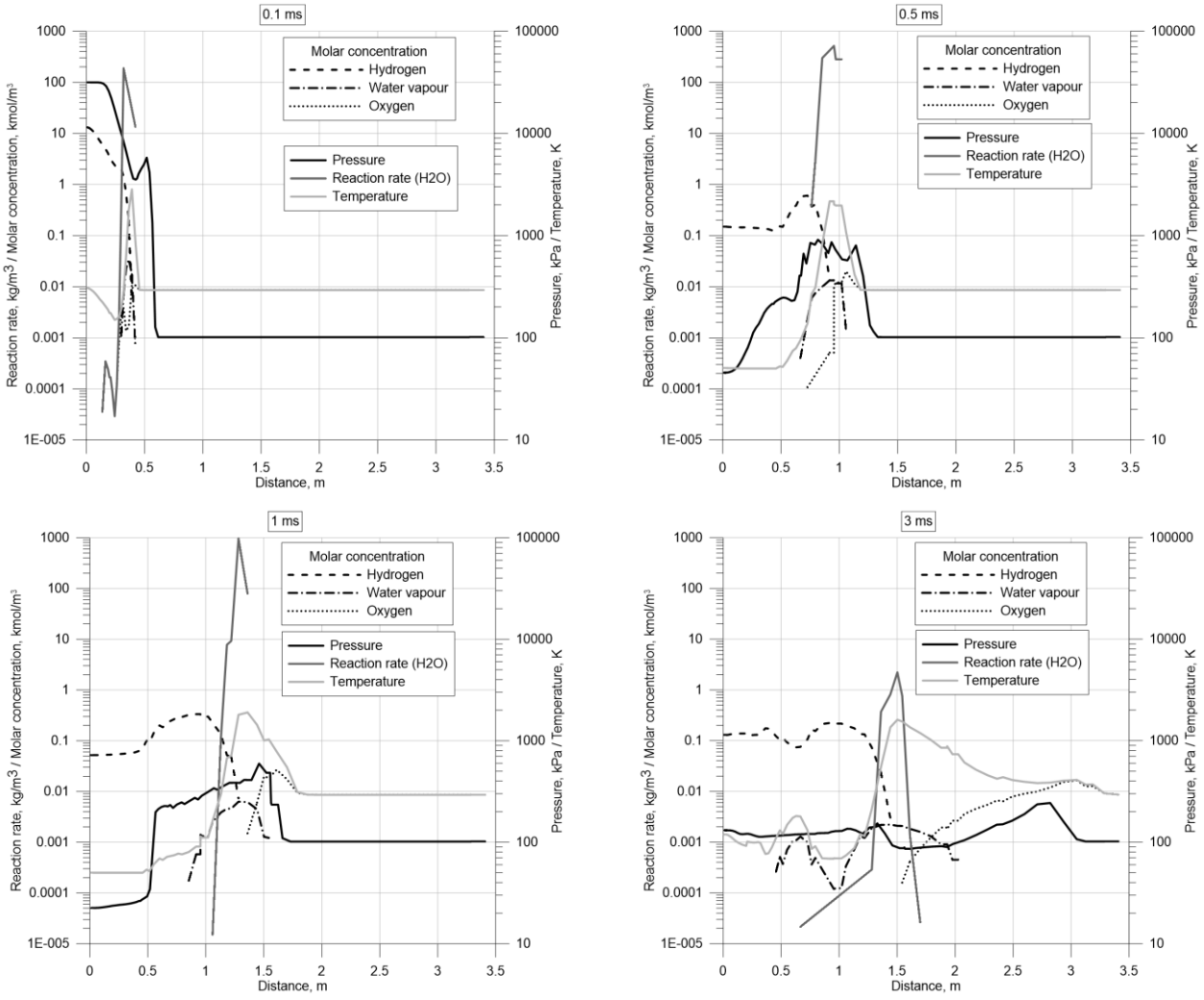

Figure 3. Molar concentrations of H2, H2O, O2, pressure and temperature distribution, and reaction rate of water generation as a function of distance perpendicular to the tank axis at time 0.1, 0.5, 1.0, and 3.0 ms (USA test)

Figure 4 demonstrates the LES model capability to reproduce well the size of experimental fireball of 7.7 m at 45 ms and its shape in the USA test.

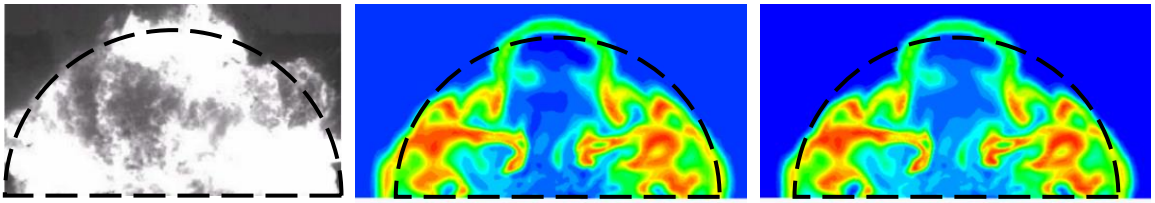

Figure 4. Experimental (left) versus simulated fireball size at time 45 ms: temperature range 149-2250 K (centre), mole fraction of H2O range 0-0.32 (right). Dashed line diameter is 7.7 m.

6 Conclusions

The originality and significance of this study are in the scientific analysis and proof of the contribution of combustion to the blast wave strength after a high-pressure hydrogen storage tank rupture in a fire. The rigor of the study is in the ability of the developed LES model to reproduce experimental data on blast wave and fireball in fire tests with 35 MPa and 70 MPa hydrogen tanks performed in USA and Japan respectively. The mechanism of combustion rate reduction in the beginning of the process is identified. The reduction of pressure at the contact surface in time is the main reason for the significant decrease of reaction rate after 1-3 ms after the tank rupture in a fire. It is shown that the amount of burned hydrogen, which contributes to the blast wave strength, increases with the growth of storage pressure.

References

[1] Dadashzadeh M, Kashkarov S, Makarov D, Molkov V. (2018). Risk assessment methodology for onboard hydrogen storage, Int. J. Hydrog. Energy, 43: 6462.

[2] Weyandt N. (2005). Analysis of Induced Catastrophic Failure of A 5000 psig Type IV Hydrogen Cylinder, Southwest Research Institute report for the Motor Vehicle Fire Research Institute, 01.06939.01.001.

[3] Zalosh R, Weyandt N. (2005). Hydrogen fuel tank fire exposure burst test. SAE Paper 2005-01–1886.

[4] Zalosh R. (2007). Blast waves and fireballs generated by hydrogen fuel tank rupture during fire exposure. Proc. 5th International Seminar on Fire and Explosion Hazards, Edinburgh, UK, 2007.

[5] Weyandt N. (2006). Vehicle bonfire to induce catastrophic failure of a 5000-psig hydrogen cylinder installed on a typical SUV. Southwest Research Institute report for the Motor Vehicle Fire Research Institute.

[6] Molkov V, Kashkarov S. (2015). Blast wave from a high-pressure gas tank rupture in a fire: Stand-alone and under-vehicle hydrogen tanks. Int. J. Hydrog. Energy, 40: 12581.

[7] Baker WE, Cox PA, Westine PS, Kulesz JJ, Strehlow RA. (1983). Explosion hazards and evaluation. Elsevier Scientific Publishing Company.

[8] Tamura Y, Takahashi M, Maeda Y, Mitsuishi H, Suzuki J, Watanabe S. (2006). Fire Exposure Burst Test of 70 MPa Automobile High-pressure Hydrogen Cylinders. Society of Automotive Engineers of Japan. Proc. Annual Autumn Congress 2006, Sapporo.

[9] Magnussen BF. (2005). The Eddy Dissipation Concept. A bridge between science and technology.